J Nanopart Res (2009) 11:15–24
DOI 10.1007/s11051-008-9417-9

Toxicity of amorphous silica nanoparticles in mouse keratinocytes

Kyung O. Yu · Christin M. Grabinski · Amanda M. Schrand · Richard C. Murdock · Wei Wang · Baohua Gu · John J. Schlager · Saber M. Hussain

Received: 22 April 2008 / Accepted: 18 May 2008 / Published online: 10 June 2008

Abstract The present study was designed to examine the uptake, localization, and the cytotoxic effects of well-dispersed amorphous silica nanoparticles in mouse keratinocytes (HEL-30). Mouse keratinocytes were exposed for 24 h to various concentrations of amorphous silica nanoparticles in homogeneous suspensions of average size distribution (30, 48, 118, and 535 nm SiO_2) and then assessed for uptake and biochemical changes. Results of transmission electron microscopy revealed all sizes of silica were taken up into the cells and localized into the cytoplasm. The lactate dehydrogenase (LDH) assay shows LDH leakage was dose- and size-dependent with exposure to 30 and 48 nm nanoparticles. However, no LDH leakage was observed for either 118 or 535 nm nanoparticles. The mitochondrial viability assay (MTT) showed significant toxicity for 30 and 48 nm at high concentrations (100 μg/mL) compared to the 118 and 535 nm particles. Further studies were carried out to investigate if cellular reduced GSH and mitochondria membrane potential are involved in the mechanism of SiO_2 toxicity. The redox potential of cells (GSH) was reduced significantly at concentrations of 50, 100, and 200 μg/mL at 30 nm nanoparticle exposures. However, silica nanoparticles larger than 30 nm showed no changes in GSH levels. Reactive oxygen species (ROS) formation did not show any significant change between controls and the exposed cells. In summary, amorphous silica nanoparticles below 100 nm induced cytotoxicity suggest size of the particles is critical to produce biological effects.

Keywords Oxidative stress · Mouse keratinocytes · Size-dependent toxicity of nanoparticles · Nanotechnology · Occupational health · EHS

K. O. Yu · C. M. Grabinski · A. M. Schrand · R. C. Murdock · J. J. Schlager · S. M. Hussain (✉)
Applied Biotechnology Branch, Human Effectiveness Directorate, Air Force Research Laboratory, Wright-Patterson AFB, Dayton, OH, USA
e-mail: saber.hussain@wpafb.af.mil

W. Wang · B. Gu
Environmental Sciences Division, Oak Ridge National Laboratory, Oak Ridge, TN, USA

Introduction

Nanotechnology is a rapidly emerging materials science area that provides man-made materials with distinctive physical properties. Nanomaterials, which have been defined as ranging in one nominal dimension from 1 to 100 nm, have been used to create unique devices possessing novel physical and chemical functional properties. Synthetic free nanoparticles are manufactured from diverse soluble and insoluble materials, with a wide range of size distributions, shapes, and modified surface functions (Ryman-Rrasnyssen et al. 2006). Silica (silicon dioxide, SiO_2) nanoparticles have great practical importance in the

fabrication of electric and thermal insulators, catalyst supports, drug carriers (Roy et al. 2005), gene delivery (Csogör et al. 2003), and media for coating processes and are also used as adsorbents, molecular sieves, and filler materials (Hoet et al. 2004). Colloidal silica crystals with periodicity within the optical wavelength scale also have a photonic band gap and thus have electronic applications ranging from microwave to optical devices (Wang et al. 2003b). The interests of silica-ordered particle arrays lie in the fact that it is possible to induce wavelength coalescence with the close-packed structure. These particle arrays can diffract light in the UV, visible, and near infrared regions in a manner analogous to X-ray diffraction from ordinary mineral crystals (Wang et al. 2003a, b). Many aspects related to the size of these materials have raised safety concerns during their production, their use in consumer products, and their eventual deposition into the environment. These aspects include biological exposure levels and availability, kinetics and dynamics of movement, and their general acute and chronic effects. Though many engineered nanoparticles could provide benefits to society, their interactions with a biological system and potential toxic/bioeffects have not been well addressed (Donaldson et al. 2004; Hardman 2006; Service 2005; Vinardell 2005).

Nanoparticles can enter the body via different routes such as the gastrointestinal tract (Zhou and Yokel 2005), lungs (Lam et al. 2004; Warheit et al. 2004), and passage through skin (Oberdoerster et al. 2005). The epidermis is an excellent barrier to protect the body from external insult; however, nanoparticles can penetrate through the broken or flexed skin (Oberdoerster et al. 2005). Nanoparticles such as TiO_2 or ZnO in sunscreens can penetrate the human stratum corneum and into some hair follicles, but not in deep layer of skin. Therefore, although the skin has been reported as non-permeable to allow passage to the organism (Lademann et al. 1999; Hoet et al. 2004), the skin and its cellular components do retain the full burden of the nanoparticulate exposure.

The objective of this study was to illustrate the acute effects of well-dispersed and different sizes of silica nanoparticles in upper layers of the skin using mouse skin epidermal cells or keratinocytes. These particles were studied due to the lack of aggregation propensity for determining cellular uptake, changes in mitochondria-based viability, membrane leakage, and oxidative stress of largely free, unagglomerated form of nanoparticulate.

Materials and methods

Chemicals

Silica nanoparticles (30, 48, 118, and 535 nm in >18 MΩ cm^{-1} deionized water) were synthesized using published methods (Wang et al. 2003a). Culture media (DMEM, F-12, Hams) and heat-inactivated fetal bovine serum (FBS) were purchased from American Type Culture Collection (ATCC, Manassas, VA). Penicillin–streptomycin, [3-(4,5-dimethylthiazol-2yl)-diphenyltetrazolium bromide], NADH, and pyruvate were obtained from Sigma Chemical Company (St. Louis, MO). 2′,7′-Dichlorofluorescein diacetate was purchased from Molecular Probes (Carlsbad, CA). The GSH kit was from Cayman Chemical Co. (Ann Arbor, MI). All other chemicals used were of the highest grade commercially available.

Zetasizer Nano ZS (Malvern Instruments)

To characterize particle sizes of silica nanoparticles in aqueous suspension, a dynamic light scattering (DLS) technique was employed using a Malvern Instruments Zetasizer Nano ZS. This device can measure particle sizes ranging from 0.6 nm to 6 μm. The particle size is correlated to measurement of dynamic fluctuations of light scatter intensity, caused by Brownian motion of the particles during movement in the aqueous liquid. This measure yields the average particle size in solution. The instrument provides data in three metrics: intensity, volume, and distribution number, which provide complete solution particle characterization. Silica nanoparticles were suspended in water and in exposure media to study the effect of different solutions on particle characterization.

Cell culture

The seed cultures of HEL-30 cells were generously provided by the Naval Health Research Center Detachment Environmental Health Effects Laboratory at Wright-Patterson AFB. These immortalized

mouse keratinocytes were used between passages 50 and 100. The cells were grown in Ham's Nutrient Mixture F-12 medium, pH 7.25, with 10% heat-inactivated FBS, and 1% antibiotic mixture of penicillin and streptomycin. Exposure media had the same components without serum. Depending on the intended toxicity assay, all the cells were seeded and grown in 6-well, 24-well, and 96-well plates and/or chambered microscope slides for 24 h until they became 80–90% confluent. The cells were maintained in a humidified incubator with 5% CO_2 at 37 °C.

Exposure

For biochemical assays, the HEL-30 cells (1×10^5 cells/mL) were seeded in a 24- or 96-well plate (Wang and Joseph 1999). Twenty-four hours after seeding the cells, they were dosed for 24 h in exposure media to different sizes of silica (SiO_2) nanoparticles (30, 48, 118, and 535 nm) at different concentrations of SiO_2 nanoparticles (0, 10, 50, 100, and 200 μg/mL). Silica NPs provided in >18 MΩ cm^{-1} deionized water were shaken in a Haake-Buchler vortexer for 5 min and made the desired concentrations with exposure media. Measurement of biochemical endpoints ($n = 3$–4 with three independent experiments) was determined by various assays described below.

For determination of silica nanoparticle uptake, cells were plated at 1×10^6 cells/mL in 6-well plates and then were grown overnight. The next day, the cells were dosed with 100 μg/mL of the various sizes of silica nanoparticles for 24 h and then processed for transmission electron microscopy (TEM) as described below. Since silica nanoparticles showed toxic effects at concentration of 100 μg/mL, the TEM experiment was carried out at this dosing level.

Transmission electron microscopy for determination of silica nanoparticle uptake into the cells

The HEL-30 cells were grown and dosed as described above. After 24 h, silica nanoparticles dosing solution was removed, and the cells were washed with phosphate buffered saline (PBS) 2× to remove unbound nanoparticles. The cells were then detached with trypsin (1% trypsin in PBS) from the 6-well plates and lightly pelleted in 15 mL conical tubes at low (500 rpm) speed. The cells were resuspended for fixation in 2.5% glutaraldehyde/formaldehyde in PBS for 2 h at room temperature. The cells were rinsed with PBS 2× and then post-fixed with 1% OsO_4 in PBS for 1 h. After rinsing with deionized water, the cells were dehydrated through an ethanol series (50%, 70%, 95%, 100%) for 15 min each followed by 1:1 dilution of 100% ethanol and LR White Resin for 1–2 h. Full embedment was accomplished with 100% resin cured at 80 °C overnight under vacuum. Thin sections (70 nm) were made from the fully cured sample block with a diamond knife on a Leica Ultracut microtome, placed onto Cu grids, and imaged using TEM (Hitachi S-7600, 100 kV).

Biochemical endpoints

Membrane integrity

Lactate dehydrogenase (LDH) is an enzyme widely present in cytosol that converts lactate to pyruvate. When plasma membrane integrity is altered or disrupted, LDH leaks into media and its extracellular levels elevate depending upon the material/chemical toxicity. Therefore, higher LDH values in the medium indicate higher toxicity levels. At the end of 24-h exposure, LDH levels in the media versus the cells were quantified and compared to the control values using a 96-well plate format and a SpectraMAX microplate reader (Molecular Devices, Sunnyvale, CA) at 340 nm according to the manufacturer's procedure.

Mitochondrial function

MTT assay was used to investigate mitochondrial function. Yellow MTT (3-(4,5-dimethylthiazol-2-yl)-2,5-diphenyltetrazolium bromide) is reduced to aqueous insoluble purple formazan by a mitochondrial enzyme showing intact functional mitochondria. Mitochondrial function of the cells was investigated spectrophotometrically after 24-h exposure to silica nanoparticles. Briefly, the culture media was removed, and fresh media containing tetrazolium salt (1:10 dilution) was added and incubated for 30 min. The media was removed and the purple formazan formed in the cells was extracted with acidic isopropyl alcohol. A SpectraMAX 190 spectrophotometer (Molecular Devices, Sunnyvale, CA) was used to determine the absorbance at 570 nm with a

reference of 690 nm to eliminate error, according to the manufacturer's procedure.

Reduced glutathione (GSH)

Reduced glutathione (GSH) possessing significant density of a free reductive thiol group for the cell is an important antioxidant for cells. During the process to remove hydrogen peroxide or lipid peroxides, GSH (reduced form) becomes oxidized to GSSG which is then recycled to GSH by the enzymes in the cells. Reduced glutathione (GSH) was measured after 24-h exposure of silica nanoparticles, using a glutathione assay kit by Cayman Chemical Company (Ann Arbor, MI). GSH levels were compared with the control values.

Reactive oxygen species (ROS)

Oxidative stress was assessed by measuring the formation of reactive oxygen species (ROS). Before dosing the cells with silica nanoparticles, the cells were treated with fluorescent probe (2′,7′-dichlorodihydrofluorescein diacetate) for 30 min under dark conditions. After removing growth media, cells were exposed to the nanoparticles for 0, 0.5, 1, 2, 4, 6, 8, 20, 24 h and tested for free radical production. Fluorescence of the cells was measured in a SpectraMax Gemini multi-well fluorescence plate reader at excitation 485 nm and emission at 530 nm.

Statistical analysis

The data were analyzed as mean ± SD of three independent experiments (each $n = 3$–4 replicates) and were further analyzed by one-way analysis of variance (ANOVA) and the Tukey–Kramer multiple comparisons test using PHStat2 software to compare exposure groups. All comparisons must meet a minimum significance level of $p < 0.05$ to indicate a significant difference.

Results

Figures 1 and 2 provide transmission electron microscope images of monodispersed silica nanoparticles in water and the average particle size with standard deviation, respectively (Wang et al. 2003a). The DLS method was used to characterize silica nanoparticle sizes shown in Table 1. No changes in particle sizes were observed in water versus dosing media with the exception of the 30 nm particle solutions, which were estimated as 28.9 nm in water and 39 nm in the media by DLS.

To verify the uptake of nanoparticles, cells were incubated with 100 μg/mL of silica nanoparticles for 24 h, followed by imaging with TEM (Fig. 3). Cells show internalization of all the different sizes of silica nanoparticles into intracytoplasmic vacuoles or endosomes. There was no evidence of silica nanoparticles in the nucleus, but they could be found randomly in the cytoplasm. Higher magnification insets of the selected areas show individual 535 nm silica nanoparticles (Fig. 3d), while all the smaller-sized silica nanoparticles (30, 48, and 118 nm) were found in loose aggregates containing multiple nanoparticles, in some instances with retention of the characteristic nanoparticle sizes and shapes (Fig. 3a–c).

The effects of silica nanoparticles on cell membrane integrity are shown in Fig. 4. At 100 μg/mL, membrane leakage of LDH was 43%, 30%, 7%, and 8% of the control, decreasing with increasing size of silica particles. The smallest size at the highest concentration (30 nm at 200 μg/mL) presented the most toxic effect as indicated by LDH measurements.

There was an inverse relationship between particle size and MTT reduction (Fig. 5) where at 200 μg/mL, only the smaller 30 and 48 nm silica particles induced significant MTT reductions of 30% and 50%, respectively (Fig. 5). At 100 μg/mL, MTT reduction in cells from exposure to 30 and 48 nm particles was 42% and 55%, respectively. The two particles in nanosizes 30–48 nm showed significant cytotoxicity, while the other two larger sizes above 100 nm (118 and 535 nm) did not show toxicity as demonstrated by MTT reduction.

Figure 6 shows an inverse correlation between LDH and MTT for cytotoxicity. There was a strong correlation ($R^2 = 0.9623$) at 200 μg/mL in various sizes of silica nanoparticles.

Experiments were performed to study redox potential/thiol status (Fig. 7). The smallest particles at high concentration of silica produced toxicity. Exposure to 30 nm particles showed GSH levels decreased to 93%, 89%, and 78% in cells exposed to 50, 100, and 200 μg/mL, respectively, when compared to controls. Only at the highest concentrations (200 μg/mL) of 30 nm silica nanoparticles, the

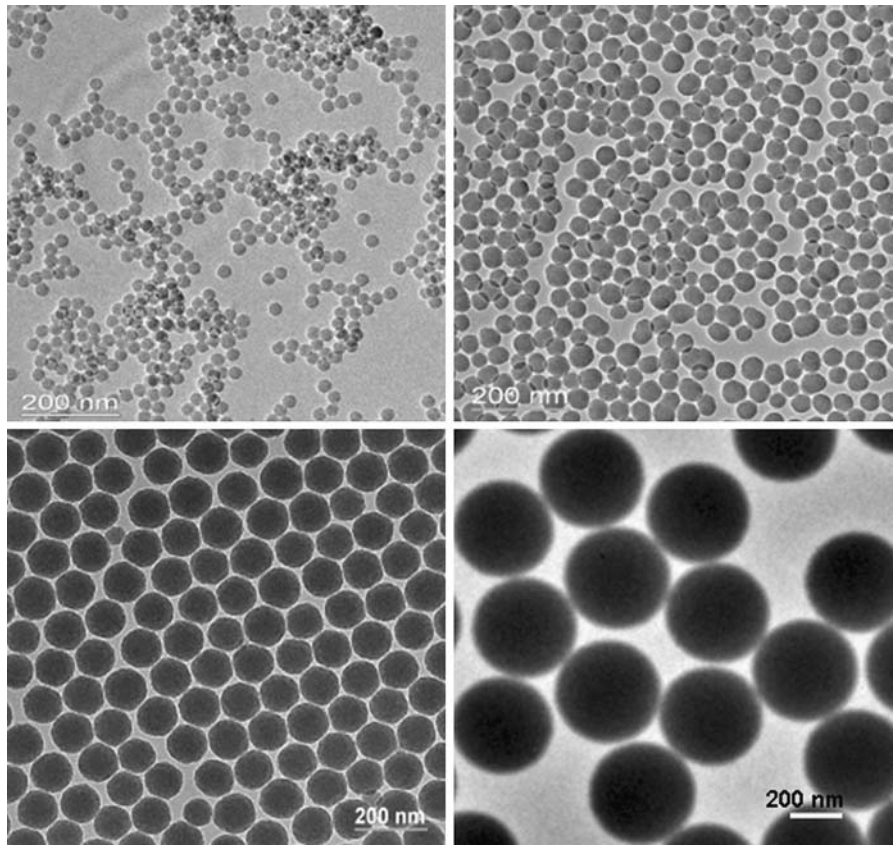

Fig. 1 Transmission electron microscope (TEM) of SiO_2 spheres

toxicity was statistically significant. There was marginal reduction of GSH level in 48 nm particulate exposed cells. No changes in GSH levels were detected at any concentration for the 118 and 535 nm nanoparticles.

Increase in ROS levels causes damage to cell structures (oxidative stress), eventually leading to cell death or apoptosis (McCabe 2003; Thibodeau et al. 2004). Time course studies of silica particles (30, 48, 118, and 535 nm) at different concentrations (0, 10, 50, 100, and 200 μg/mL) were performed, and no significant increase of ROS levels was observed at any time point or at any concentration when compared with the controls (Fig. 8).

Discussion

In order to study toxicity of nanoparticles, it is imperative to know exact size, shapes, and physical properties including the aggregation/agglomeration/dispersion properties of nanoparticles in culture media. Therefore, characterization of nanoparticles should be performed initially and throughout as needed for studies for assuring particle dynamics and dosing size and type. Uniform dispersal of particles allows for controlling the size element and surface area components of nanoparticulate for determining size-dependent data in toxicity measurements (Jillavenkatesa and Kelly 2002; Vertegel et al. 2004). Recently, we investigated comprehensive characterization of aggregated and agglomerated nanoparticles in solution and relevance to toxicity using a cell culture system (Murdock et al. 2008). Powers et al. (2006) reported many techniques to determine the size of nanoparticles, such as DLS, centrifugal sedimentation, laser diffraction/static light scattering, low pressure impactor, size exclusion chromatography, electron microscopy, time of flight mass spectroscopy, and atomic force microscopy. In the present study, two methods were used for the critical measurement of size variations, TEM, and DLS. The data (Table 1)

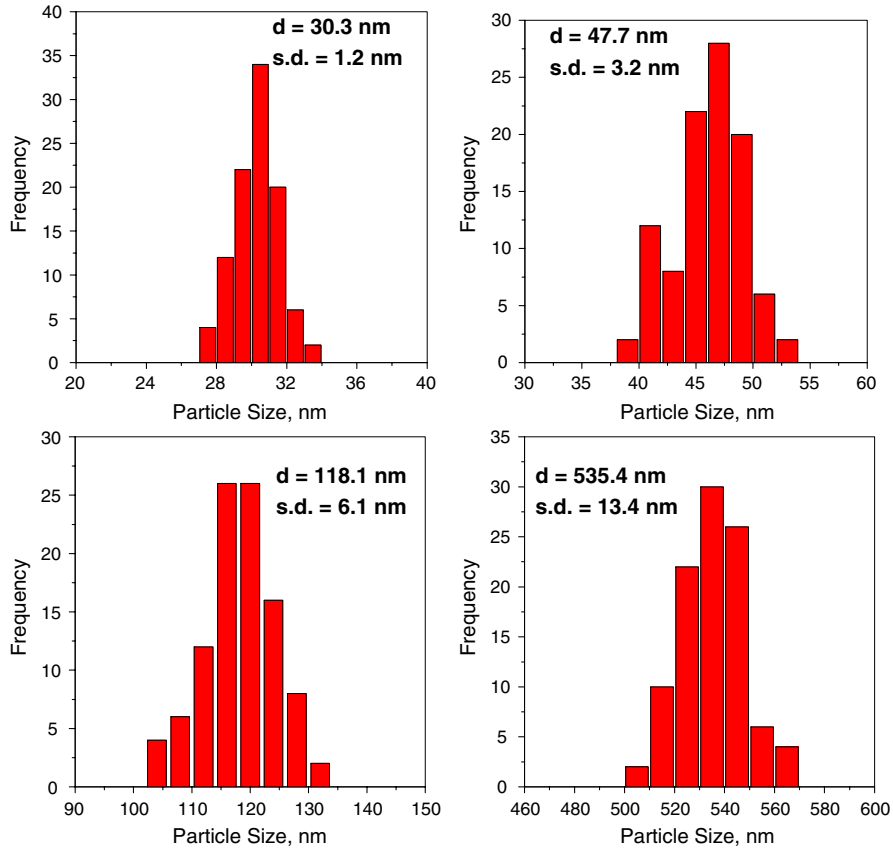

Fig. 2 The average particle size (d) and the standard deviation were determined by analyzing over 300 particles

Table 1 Particle sizes of silicon dioxide in water and in dosing media measured by dynamic light scattering device which produced similar results studied by the electron microscope

Particle	Instrumentation (DLS)		Microscope (TEM)	
	Average diameter (nm)	PDI	Average diameter (nm)	SD
SiO_2 A				
Water	28.9	0.093	30.3	1.2
Media	39.0	0.116	na	na
SiO_2 B				
Water	52.9	0.07	47.7	3.2
Media	51.9	0.069	na	na
SiO_2 C				
Water	121	0.007	118	6.1
Media	119	0.018	na	na
SiO_2 D				
Water	537	0.438	535	13.4

shows that both techniques gave a similar result for silica nanoparticles size when suspended in water. Particle sizes used in this study were received as 30, 48, 118, and 535 nm based on synthesis and characterized by DLS in two different laboratories. Since the cells were dosed with silica nanoparticles in exposure media, it was critical to ensure that there would be no changes in nanoparticles characteristics when they were suspended in media. Except for the largest particle (535 nm), data from DLS indicates no changes

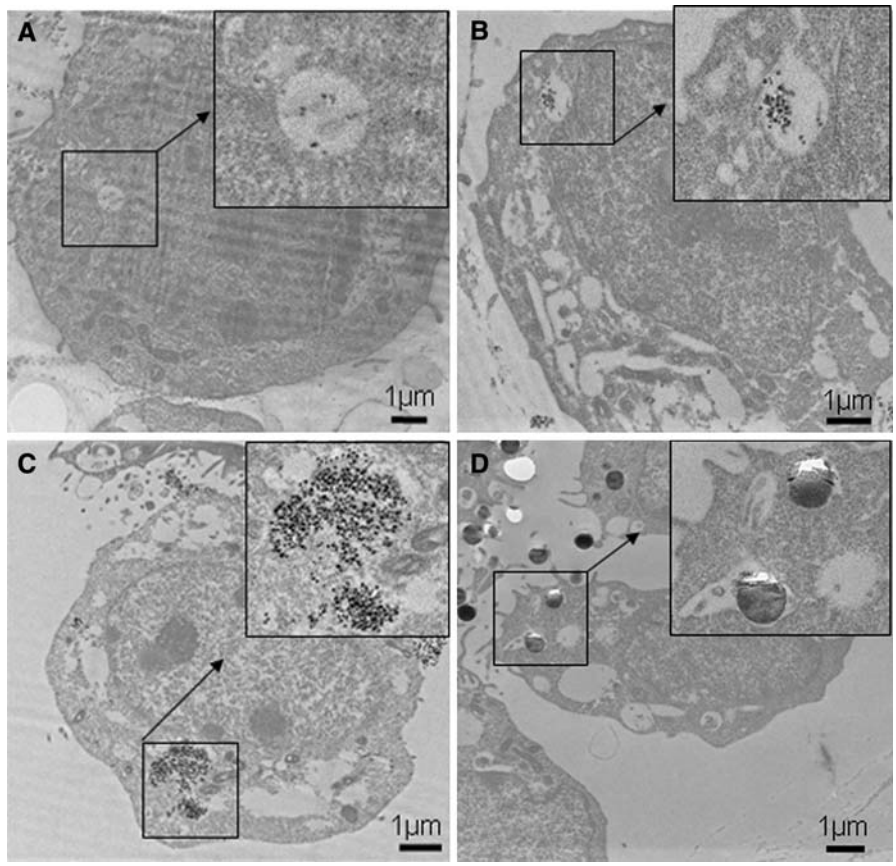

Fig. 3 Transmission electron microscopy (TEM) of HEL-30 cells incubated with 100 μg/ml of silica nanoparticles for 24 h showing internalization of all sizes used in this study: (**a**) 30 nm SiO_2, (**b**) 48 nm SiO_2, (**c**) 118 nm SiO_2, and (**d**) 535 nm SiO_2. Boxes provide higher magnification images correspond to the areas inside the box

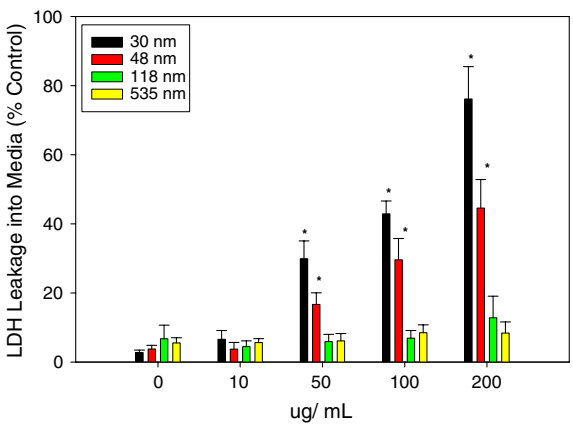

Fig. 4 Effect of SiO_2 on LDH leakage into media (% control). The HEL-30 cells were dosed with different sizes (30, 48, 118, and 535 nm) and various concentrations of silica (0, 10, 50, 100, and 200 μg/mL) for 24 h. Size- and dose-dependent LDH leakage were observed in 30 and 48 nm silica nanoparticles. Large size (118 and 535 nm) showed less toxicity compared with smaller nanoparticles. Three independent experiments ($n = 3$) were carried out, and data are means ± SD. * Significantly different from control at $p < 0.05$

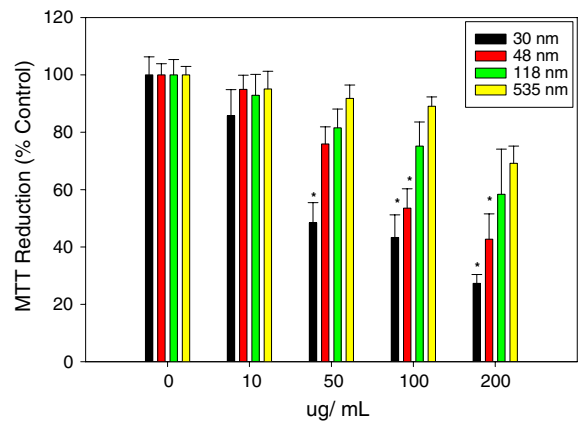

Fig. 5 Effect of silica nanoparticles on MTT reduction (% control). The HEL-30 cells were dosed with different sizes (30, 48, 118, and 535 nm) and various concentrations of silica (0, 10, 50, 100, and 200 μg/mL) for 24 h. Size- and dose-dependent MTT reduction in 30 and 48 nm at higher concentrations (200 μg/mL) produced significant toxicity when compared to large sizes (118 and 535 nm). Three independent experiments ($n = 4$) were carried out, and data are means ± SD. * Significantly different from control at $p < 0.05$

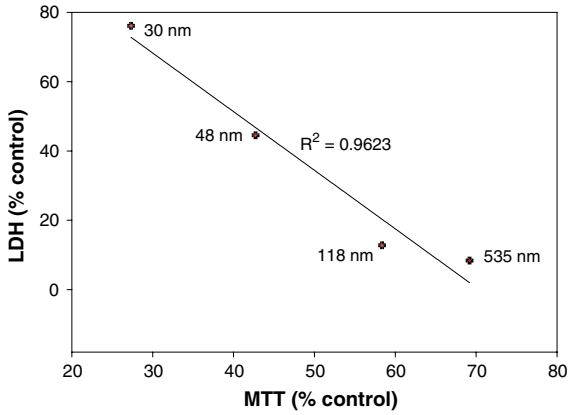

Fig. 6 Correlation between LDH and MTT in various sizes of silica nanoparticles at 200 μg/mL. Graph was generated using two data points in the highest exposure condition (200 μg/mL) in Figs. 4 and 5

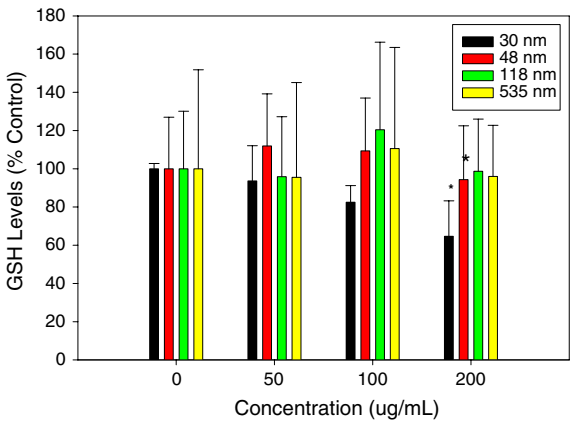

Fig. 7 Effect of silica nanoparticles on GSH levels (% control). The HEL-30 cells were dosed with different sizes (30, 48, 118, and 535 nm) and various concentrations of silica (0, 10, 50, 100, and 200 μg/mL) for 24 h. Size- and dose-dependent toxicity was observed. Three independent experiments ($n = 4$) were carried out, and data are means ± SD. * Significantly different from control at $p < 0.05$

in sizes occur when suspended in exposure media. The polydispersity index (PDI) indicates the range of sizes in a distribution of particles in solution. The largest size (535 nm) shows the highest PDI value of 0.428, while the remaining particles had smaller values, indicating more uniform dispersion. In addition, sample D (535 nm) had the largest standard deviation (13.4). Silica nanoparticles used in our experiments were spherical and dispersed homogeneously in water (Fig. 1). However, it may be possibly that some nanoparticles formed transient aggregates in

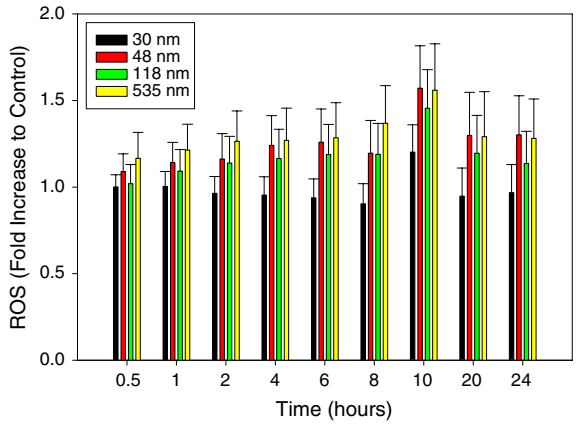

Fig. 8 Time course study of effect of silica nanoparticles on ROS formation (fold of increase compared with the control). The HEL-30 cells were dosed with different sizes (30, 48, 118, and 535 nm) and various concentrations of silica (0, 10, 50, 100, and 200 μg/mL) for 0, 0.5, 1, 2, 4, 6, 8, 10, 20, and 24 h. There was no difference between the controls and dosed cells. Concentration of 10 μg/mL was selected to represent this study. There was no difference statistically in all experiments

solution due to Van der Waals forces and hydrophobic interaction from solute media surface coating that formed larger than the original particles.

After the mouse keratinocytes were incubated with 100 μg/mL of silica nanoparticles in exposure media for 24 h, all sizes of the particles were found to be taken up into the cytoplasm of the cells. This suggests that the nanoparticles came into direct contact with the cell membrane and were subsequently internalized during this time period. The apparent aggregation or agglomeration of the smaller-sized nanoparticles (30, 48, 118 nm) inside the intracellular vacuoles may be an artifact of the mechanism of internalization (i.e., endocytosis, phagocytosis) and is not likely to be representative of the nanoparticle aggregates state outside of the cells, which were not detected. This hypothesis is further supported by the DLS studies demonstrating the presence of individual silica nanoparticles in suspension and the fact that individual 535 nm nanoparticles may be uptaken singly due to their large size. Although the TEM images verify the uptake of silica nanoparticles into the cells, the method is not able to determine the cumulative or quantitative amount of silica nanoparticle taken up at each size. Further studies are underway to correlate the kinetics of uptake (size versus time) with cytotoxicity. Nel et al. (2006) reported the inverse

relationship between particle size and number of surface molecules. More atoms or molecules are expressed on the surface of the smaller size particles (30 nm), and biological activity could be determined by this. Oberdoerster et al. (2005) also reported that particles with greater specific surface area per mass are more active biologically. Our results confirm that the smaller silica nanoparticles with more specific surface area show more toxic effects.

Thibodeau et al. (2004) studied silica-induced apoptosis in the mouse alveolar macrophages to investigate lung disease characterized by pulmonary fibrosis. The authors reported that mitochondrial depolarization and caspase 3 and 9 activation contributed to apoptosis when the cells were exposed to silica. The role of ROS was investigated in their study, but it was not apparent. Our work in mouse keratinocytes revealed that toxicity of silica nanoparticles does not seem to be initiated through ROS overproduction. Brown et al. (2007) dosed normal human methothelial cells with 100 nm silica spheres at the concentration of 26.7 μg/mL and reported LDH leakage as 3% after 24 h exposure. Results of our study in mouse keratinocytes were very similar to their findings (Fig. 5). Membrane integrity and mitochondrial function by LDH and MTT show size-dependent toxicity, which could be due to the increased specific surface area for decreasing nanoparticle size (Lin et al. 2006).

There was no statistically significant difference between the control and the treated groups for reduced glutathoine levels. However, only the smallest size (30 nm) at the most toxic dose, 200 μg/mL, resulted in reduced glutathione levels. Although many other studies have shown that nanoparticles may produce toxicity by generating ROS, in this study, silica nanoparticles of different sizes did not produce significantly different ROS generation from the control when using the fluorescent dichlorofluorescein probe. Therefore, direct physical disruption of membranes through materials interaction or another unknown mechanisms may be at work to produce size-dependent toxicity. Further work on nanoparticles is warranted before they can be considered safe for a casual exposure.

Acknowledgments The authors like to thank Col J. Riddle for his strong support and encouragement for this research. Our thanks also go to Paul Bloomer and Richard Freeman for their computer support. This work was supported by the Air Force Office of Scientific Research (AFOSR) Project (BIN# 2312A214).

References

Brown SC, Kamal M, Nasreen N, Baumuratov A, Sharma P, Anthony V, Moudgil BM (2007) Influence of shape, adhesion and simulated lung mechanics on amorphous silica nanoparticle toxicity. Adv Powder Technol 18:69–79

Csogör ZS, Nacken M, Sameti M, Lehr C-M, Schmidt H (2003) Modified silica particles for gene delivery. Mater Sci Eng C 23:93–97

Donaldson K, Stone V, Tran CL, Kreyling W, Borm PJA (2004) Nanotoxicology. Occup Environ Med 61:727–728

Hardman R (2006) A toxicologic review of quantum dots: toxicity depends on physicochemical and environmental factors. Environ Health Perspect 114:165–172

Hoet PHM, Brueske-Hohlfeld I, Salata O (2004) Nanoparticles—known and unknown health risks. J Nanotoxicol 2:1–2

Jillavenkatesa A, Kelly JF (2002) Nanopowder characterization: challenges and future directions. J Nanopart Res 4:463–468

Lademann J, Weigmann H, Rickmeyer C, Barthelmes H, Schaefer H, Mueller G, Sterry W (1999) Penetration of titanium dioxide microparticles in a sunscreen formulation into the horny layer and the follicular orifice. Skin Pharmacol Appl Skin Physiol 12:247–256

Lam C-W, James JT, McClustkey R, Hunter R (2004) Pulmonary toxicity of single-wall carbon nanotubes in mice 7 and 90 days after intratracheal instillation. Toxicol Sci 77:126–134

Lin W, Huang Y-W, Zhou X-D, Ma Y (2006) In vitro toxicity of silica nanoparticles in human lung cancer cells. Toxicol Appl Pharmacol 217:252–259

McCabe MJ Jr (2003) Mechanisms and consequences of silica-induced apoptosis. Toxicol Sci 76:1–2

Murdock RC, Braydich-Stolle L, Schrand AM, Schlager JL, Hussain SM (2008) Characterization of nanomaterial dispersion in solution prior to in vitro exposure via dynamic light scattering. Toxicol Sci 101:239–253

Nel A, Xia T, Maedler L, Li N (2006) Toxic potential of materials at the nanolevel. Science 311:622–626

Oberdoerster G, Oberdoerster E, Oberdoerster J (2005) Nanotoxicology: an emerging discipline evolving from studies of ultrafine particles. Environ Health Perspect 113:823–839

Powers KW, Brown SC, Krishna VB, Wasdo SC, Modgil BM, Roberts SM (2006) Research strategies for safety evaluation of nanomaterials. Part VI. Characterization of nanoscale particles for toxicological evaluation. Toxicol Sci 90:296–303

Roy I, Ohulchanskyy T, Bharali D, Pudavar H, Mistretta R, Kaur N, Prasad P (2005) Optical tracking of organically modified silica nanoparticles as DNA carriers: a nonviral, nanomedicine approach for gene delivery. PNAS 102: 279–284

Ryman-Rrasnyssen JP, Riviere JE, Monteiro-Riviere NA (2006) Penetration of intact skin by quantum dots with diverse physicochemical properties. Toxicol Sci 91:159–165

Service R (2005) Calls rise for more research on toxicology of nanomaterials. Science 310:1609

Thibodeau M, Giardina C, Knecht DA, Helble J, Hubbare AK (2004) Silica-induced apoptosis in mouse alveolar macrophages is initiated by lysosomal enzyme activity. Toxicol Sci 80:34–48

Vinardell MP (2005) In vitro cytotoxicity of nanoparticles in mammalian germ-line stem cell. Toxicol Sci 88:285–286

Vertegel AA, Aiegel RW, Dordick JS (2004) Silica nanoparticle size influences the structure and enzyme activity of adsorbed lysozyme. Langmuir 20:6800–6807

Wang H, Joseph JA (1999) Quantitating cellular oxidative stress by dichlorofluorescein assay using microplate reader. Free Radic Biol Med 27:612–616

Wang W, Gu B, Liang L, Hamilton W (2003a) Fabrication of two- and three-dimensional silica nanocolloidal particle arrays. J Phys Chem B 107:3400–3404

Wang W, Gu B, Liang L, Hamilton W (2003b) Fabrication of near infrared photonic crystals using highly-monodispersed submicrometer SiO_2 spheres. J Phys Chem B 107: 12113–12117

Warheit DB, Laurence BR, Reed KL, Roach DH, Reynolds GAM, Weff TR (2004) Comparative pulmonary toxicity assessment of single-wall carbon nanotubes in rats. Toxicol Sci 77:117–125

Zhou Y, Yokel R (2005) The chemical species of aluminum influence its paracellular flux and uptake into Caco-2 cells, a model of gastrointestinal absorption. Toxicol Sci 87:15–26